Published in final edited form as:
Matrix Biol. 2009 May ; 28(4): 211–220. doi:10.1016/j.matbio.2009.03.004.

Analysis of Dermal Elastic Fibers in the Absence of Fibulin-5 Reveals Potential Roles for Fibulin-5 in Elastic Fiber Assembly

Jiwon Choi[1], **Andreas Bergdahl**[1], **Qian Zheng**[2], **Barry Starcher**[3], **Hiromi Yanagisawa**[2], and **Elaine C. Davis**[1,*]

1 *Department of Anatomy and Cell Biology, McGill University, Montreal, QC, Canada, H3A 2B2*

2 *Department of Molecular Biology, University of Texas Southwestern Medical Center, Dallas, TX, USA*

3 *Department of Biochemistry, University of Texas Health Center, Tyler, TX, USA*

Abstract

Fibulin-5 is a 66 kDa modular, extracellular matrix protein that localizes to elastic fibers. Although *in vitro* protein-protein binding studies have shown that fibulin-5 binds many proteins involved in elastic fiber formation, the specific role of fibulin-5 in elastogenesis remains unclear. To provide a more detailed analysis of elastic fiber assembly in the absence of fibulin-5, the dermis of wild-type and fibulin-5 gene knockout (*Fbln5*$^{-/-}$) mice was examined with electron microscopy (EM). Although light microscopy showed apparently normal elastic fibers near the hair follicles and the absence of elastic fibers in the intervening dermis of the *Fbln5*$^{-/-}$ mouse, EM revealed the presence of aberrantly assembled elastic fibers in both locales. Instead of the elastin being incorporated into the microfibrillar scaffold, the elastin appeared as globules juxtaposed to the microfibrils. Desmosine analysis showed significantly lower levels of mature cross-linked elastin in the the *Fbln5*$^{-/-}$ dermis, however, gene expression levels for tropoelastin and fibrillin-1, the major elastic fiber components, were unaffected. Based on these results, the nature of tropoelastin cross-linking was investigated using domain specific antibodies to lysyl oxidase like-1 (LOXL-1). Immunolocalization with an antibody to the N-terminal pro-peptide, which is cleaved to generate the active enzyme, revealed abundant staining in the *Fbln5*$^{-/-}$ dermis and no staining in the wild-type dermis. Overall, these results suggest two previously unrecognized functions for fibulin-5 in elastogenesis; first, to limit the extent of aggregation of tropoelastin monomers and/or coacervates and aid in the incorporation of elastin into the microfibril bundles, and second, to potentially assist in the activation of LOXL-1.

Keywords

elastic fibers; elastin; fibulin-5; lysyl oxidase like-1; skin

1. INTRODUCTION

Elastic fibers are an abundant and integral part of many extracellular matrices and are especially critical for providing the property of elastic recoil to tissues such as major blood vessels, lung and skin. In the skin, elastic fibers form an intricate network throughout the dermis, interposed

*Address for correspondence: Elaine C. Davis, Ph.D., Department of Anatomy and Cell Biology, McGill University, 3640 University Street, Montreal, Quebec, Canada H3A 2B2, phone: 514-398-5893, fax: 514-398-5047, E-mail: E-mail: elaine.davis@mcgill.ca.

between, and associated with, the hair follicles (Dahlback et al., 1990; Starcher et al., 2005). The significance of elastic fibers for normal skin development and function is clearly reflected by the numerous human conditions in which a skin phenotype occurs as a result of elastic fiber abnormalities. Examples include, cutis laxa (Uitto and Pulkkinen, 2002; Urban et al., 2005), Costello syndrome (Hennekam, 2003), mid-dermal elastolysis (Patroi et al., 2003), pseudoxanthoma elasticum (Uitto et al., 2001), papular elastorrhexis (Buechner and Itin, 2002), elastoderma (Yen et al., 1995), Buschke-Ollendorff syndrome (Giro et al., 1992) and scleroderma (Davis et al., 1999).

Morphologically, elastic fibers consist of two distinct components that are easily recognized by electron microscopy (EM); a core of amorphous-appearing elastin and a peripheral mantle of 10 nm fibrillin-containing microfibrils (Mecham and Davis, 1994; Parks et al., 1993; Rosenbloom et al., 1993). Microfibrils can exist independent of elastin, such as in the ciliary zonule, however, insoluble elastin is never observed in the absence of microfibrils. During fetal development, microfibril bundles form first and then appear to act as a scaffold for the deposition, orientation and assembly of the 70 kDa tropoelastin monomers (Mecham and Davis, 1994). Following secretion, the tropoelastin monomers are thought to coacervate, or self-assemble, forming small coacervates which then mature into slightly larger aggregates. These aggregates then become integrated into microfibril bundles and subsequently cross-linked into an insoluble elastin polymer by the extracellular enzymes lysyl oxidase (LOX) and lysyl oxidase like-1 (LOXL-1) (Kagan, 1986; Kagan and Trackman, 1991).

Although this assembly process appears relatively straightforward, the temporal and specific protein-protein interactions, and the molecular basis of how the fiber assembles, remain uncertain. Adding to the complexity of this process is the ever increasing number of elastic fiber-associated proteins that have been localized to elastic fibers or identified as elastin- and/or microfibril-binding proteins (Kielty, 2006). Recently, gene ablation studies on some of these proteins have allowed for the identification of several key players that are required for normal elastic fiber assembly (Nakamura et al., 2002; Yanagisawa et al., 2002; Liu et al., 2004; McLaughlin et al., 2006; Zacchingna et al., 2006; Dabovic et al., 2009). The specific role(s) and molecular interactions of these proteins in the assembly process, however, have yet to be completely defined.

Fibulin-5 was discovered by two groups in an attempt to isolate novel factors involved in vascular development (Kowal et al., 1999; Nakamura et al., 1999). The fibulin-5 gene (*Fbln5*) was found to be strongly expressed in vascular smooth muscle cells (SMCs) in the fetal arterial system but downregulated in most adult vascular beds (Kowal et al., 1999). Expression could be reactivated in the adult during neointima formation following vascular injury and in vascular disease (Kowal et al., 1999; Spencer et al., 2005). Taken together, these data suggested that fibulin-5 is an important regulator of vascular development.

To better define the role of fibulin-5 in the vasculature, a *Fbln5* knockout mouse model was generated. As anticipated, the fibulin-5 null mouse showed several vascular defects, including aberrant assembly of the elastic laminae in the great vessels, vascular tortuosity and an abnormal degree of cutaneous vascular sprouting (Nakamura et al., 2002; Sullivan et al., 2007; Yanagisawa et al., 2002). However, the $Fbln5^{-/-}$ mouse also showed emphysematous lungs with defective elastic fibers and severe loose skin with a remarkable near absence of dermal elastic fibers thereby indicating a more universal role for fibulin-5 as critical mediator of elastogenesis in all tissues.

Functionally, fibulin-5 has been reported to bind several integrins (Nakamura et al., 2002) and mediate endothelial cell and SMC attachment via an RGD motif contained within the first calcium binding epidermal growth factor-like domain (Lomas et al., 2007; Nakamura et al.,

2002). Recent evidence suggests that integrin binding by fibulin-5, however, does not result in receptor activation (Lomas et al., 2007) and may therefore serve as more of a physical link. Fibulin-5 can also bind tropoelastin (Yanagisawa et al., 2002), fibrillin-1 (Freeman et al., 2005; El-Hallous et al., 2007; Kobayashi et al., 2007) and LOXL-1 (Liu et al., 2004; Hirai et al., 2007), thus placing it in a distinct position to facilitate interactions between these molecules. Based on the known binding interactions identified for fibulin-5, several models have been proposed for how fibulin-5 participates in the assembly of elastic fibers. However, elastic fiber assembly *in vivo* is a complex spatially and temporally regulated process, and since most of the binding data has been obtained using solid-phase bindings assays with purified proteins and/or co-immunoprecipitation pull-down experiments, it has remained difficult to accurately predict the *in vivo* function for fibulin-5.

In an attempt to better understanding of the role of fibulin-5 in elastic fiber assembly, we sought to determine how the absence of fibulin-5 altered the assembly and ultrastructure of elastic fibers *in vivo*. For this study, the dermis was chosen since this tissue showed the most striking defect in elastic fiber assembly in the *Fbln5*$^{-/-}$ mouse. The results that we present provide novel insights into the role of fibulin-5 as a critical regulator of elastogenesis.

2. RESULTS

2.1. Light microscopic and biochemical analyses of the dermis

To analyse the specific distribution of elastin in the dermis of *Fbln5*$^{-/-}$ mice, Hart's staining for elastin was performed on *en face* sections of skin from 2 month-old wild-type and *Fbln5*$^{-/-}$ mice. Wild-type skin showed an elaborate network of long elastic fibers interconnecting and spanning between the hair follicles (Fig. 1A). In the absence of fibulin-5, only a very few, short elastic fibers could be seen in the papillary dermis, primarily near the hair follicles (Fig. 1B, arrows). Additionally, we noted the presence of very small, Hart's stained foci scattered throughout the dermis more distant from the hair follicles (Fig. 1B, arrowheads). Despite the obvious disruption of elastic fiber assembly in the *Fbln5*$^{-/-}$ mouse skin, small blood vessels located primarily at the dermal-hypodermal junction appeared very similar to wild-type vessels, both showing a prominent layer of elastin organized in longitudinal fibers immediately subjacent to the endothelium (Figs. 1C, D). Closer examination of these vessels, however, revealed a relative absence of elastic fibers within the medial and adventitial layers of the *Fbln5*$^{-/-}$ vessels. Consistent with the presence of small, fragmented elastic fibers being found in the *Fbln5*$^{-/-}$ dermis, and the considerable amount of elastin located in the vasculature, full-thickness *Fbln5*$^{-/-}$ skin biopsies in young animals (14 days) showed only reduced amounts of desmosine, a specific measure of mature cross-linked elastin (Fig. 1E). This reduced level of desmosine was significantly different from both wild-type and *Fbln5*$^{+/-}$ skin, and consistent with data from older animals (3 months) (Zheng et at., 2007).

2.2. Electron microscopic analysis of dermal elastic fiber ultrastructure

The virtual absence of elastic fibers in the dermis of fibulin-5 null mice raised two important questions. First, are the elastic fibers that do form near the hair follicles ultrastructurally normal, and second, in the regions of the dermis devoid of elastic fibers, are microfibril bundles present? By EM, elastic fibers consisting of a core of amorphous-appearing elastin surrounded by a peripheral mantle of microfibrils were easily recognized near the dermal hair follicles in wild-type mice (Figs. 2A, B). In contrast, elastic fibers that formed immediately adjacent to the hair follicles in the absence of fibulin-5 showed a clear disconnect between the microfibril bundles and the elastin (Figs. 2C, D). Additionally, the elastin itself did not form a solid mass but rather was assembled into discrete globular units of relatively uniform size. Despite the fact that the elastin did not integrate into the microfibril bundle, the two components of the elastic fiber were always found to be in close proximity. Interestingly, the internal elastic lamina (IEL) of

the small blood vessels seen in the *Fbln5*$^{-/-}$ dermis, which appeared normal by Hart's staining (Fig. 1D), also showed a similar irregular appearance by EM (data not shown), suggesting a generalized assembly defect.

In wild-type mice, elastic fibers in the dermis located at a distance from the hair follicles were identical to those found adjacent to the hair follicles, only larger (data not shown). Although Hart's staining showed no elastic fibers in this region of the *Fbln5*$^{-/-}$ skin, EM analysis revealed large bundles of microfibrils associated with collections of elastin deposits (Figs. 2E, F) and extensive microfibril bundles devoid of elastin (Fig. 2G). Close examination of these microfibril bundles revealed the occasional presence of very small elastin deposits within the bundles (Figs. 2E, G, arrowheads). Statistical analysis of the dimensions of the large elastin deposits showed them to be approximately 160 nm in diameter with substantial variation in size (Fig. 2H). In contrast, the small globules of elastin seen near the hair follicles (Figs. 2C, D) were significantly smaller at only 30 nm in diameter, with considerably less size variation (Fig. 2H). Both the small elastin globules and larger elastin deposits were consistently observed in the *Fbln5*$^{-/-}$ dermis from 14 days to 1 year of age.

2.3. Gene expression analysis

Elastic fiber assembly involves an initial self-assembly step where tropoelastin monomers coacervate, followed by the integration of small assemblies of coacervates into a fibrillin-rich microfibrillar scaffold, and subsequent cross-linking by LOX enzymes. To determine if the expression of any of these molecules was altered due to the absence of fibulin-5, quantitative real-time PCR (qPCR) was conducted on 7 day-old skin from wild-type and fibulin-5 null mice. Seven day-old skin was chosen because the gene expression of many of the elastic fiber proteins is most active in mouse skin at this age (Zheng et al. 2007). Results showed no significant difference in gene expression for elastin, fibrillin-1 and -2, and fibulin-1 and -3. However, a significant increase in gene expression was observed for fibulin-2 and -4, and LOX and LOXL-1, when fibulin-5 was absent (Fig. 3).

2.4. Localization of tropoelastin

From the qPCR data, no alteration in elastin gene expression as a consequence of the absence of fibulin-5 in the skin was apparent. However, both ultrastructural observations and biochemical data, indicated reduced formation of mature elastic fibers. Thus, to determine if tropoelastin monomers were actually present in the tissue but either not assembled into recognizable elastic fibers or too small for routine EM detection, immunostaining was carried out with an antibody that recognizes both mature elastin and tropoelastin monomers (Kozel et al., 2003; Hirano et al., 2007). As expected, immunofluorescence localization of tropoelastin/elastin in wild-type skin showed the presence of elastic fibers interconnecting the hair follicles (Fig. 4A). By EM, immunogold labeling for tropoelastin/elastin showed the presence of gold particles decorating the solid, central core of the wild-type elastic fibers with no labeling of the peripheral microfibrils (Fig. 4B). Immunofluorescence staining for tropoelastin/elastin in the *Fbln5*$^{-/-}$ skin was identical to that seen with Hart's staining, showing stunted elastic fibers near the hair follicles and confirming the presence of elastin in small foci in the intervening dermis (Fig. 4C). No generalized diffuse staining of the dermis was observed. This result was confirmed at the EM level where only the small globules (Fig. 4D) and large elastin deposits (Fig. 4E) labeled for tropoelastin/elastin, and no gold particles were observed on the 'bare' microfibrils (Figs. 4D, E).

2.5. Localization of lysyl oxidase enzymes

To fully understand the nature of the defective elastic fibers seen in the dermis of *Fbln5*$^{-/-}$ mice, the tropoelastin cross-linking enzyme LOXL-1 was localized using antibodies that are specific for either the N- or C-terminus of the protein (Liu et al., 2004). The N-terminal antibody

was raised against a sequence in the pro-peptide, which is cleaved to generate the active enzyme, and thus, this antibody only recognizes inactive LOXL-1 or the cleaved pro-peptide. The peptide used to raise the C-terminal antibody was located in the active enzyme and therefore can not distinguish between inactive and active LOXL-1. In wild-type skin, immunolabeling with the C-terminal antibody showed LOXL-1 staining in a filamentous network between adjacent hair follicles and within the papillary dermis between the hair follicles and epidermis (Fig. 5A). In contrast, the same antibody showed a distinct punctate staining pattern in the *Fbln5*$^{-/-}$ skin which was distributed throughout the papillary dermis (Fig. 5B). With the N-terminal antibody, no immunostaining was observed in wild-type skin indicating that all of the LOXL-1 labeling observed with the C-terminal antibody represented active enzyme (Fig. 5C). In the *Fbln5*$^{-/-}$ skin, a punctate pattern of staining was again seen between the epidermis and hair follicles (Fig. 5D) and deeper in the dermis between the individual hair follicles (Fig. 5D′) after immunostaining with the N-terminal antibody. Since the amount of staining appeared similar with both the N- and C-terminal antibodies, it can be reasoned that a large proportion of the LOXL-1 in the *Fbln5*$^{-/-}$ skin was likely inactive. Alternatively, some of the N-terminal pro-peptides, upon cleavage, may have remained associated with the elastic fibers in the fibulin-5 null skin and thus detected by the antibody.

To determine the specific localization of the enzyme, immunogold labeling was conducted at the EM level. With the C-terminal antibody, elastic fibers in wild-type skin showed gold particles localized at the edges of the elastin core and where the microfibrils were embedded within the core (Fig. 5E). In the *Fbln5*$^{-/-}$ skin, no labeling with the C-terminal antibody was seen on the small elastin globules (Fig 5F), but numerous gold particles were seen to decorate the large elastin deposits (Fig 5G). Consistent with the immunofluorescence data, virtually no gold particles were seen by immunogold labeling for the N-terminal of LOXL-1 on wild-type elastic fibers (Fig. 5H). In the *Fbln5*$^{-/-}$ skin, immunogold labeling for the N-terminus of LOXL-1 was also absent on the small elastin globules (Fig. 5I). However, abdundant gold particles were seen on the large elastin deposits indicating the presence of considerable inactive LOXL-1 and/or the presence of the cleaved pro-peptide within the elastin deposits in the *Fbln5*$^{-/-}$ skin (Fig. 5J).

3. DISCUSSION

In 2002, Yanagisawa et al. (2002) and Nakamura et al. (2002) simultaneously reported that, amongst other elastic fiber-related defects, *Fbln5*$^{-/-}$ mice showed incredibly lax skin with a complete loss of elastic recoil. Light microscope images showed apparently normal elastic fibers around the hair follicles and a complete absence of elastic fibers in the intervening dermis. Based on these observations and the regional discrepancy in the ability of elastic fibers to form, it was difficult to propose a mechanistic role for fibulin-5 in elastic fiber assembly. In the present study, EM was used to definitively characterize the ultrastructure of dermal elastic fibers formed in the absence of fibulin-5. Only with the resolution afforded by this technique, were we able to determine that the presumed normal elastic fibers seen adjacent to the hair follicles were indeed defective and that the areas thought to be devoid of elastic fibers did contain elastic fiber components, albeit incorrectly assembled.

In the absence of fibulin-5, the elastic fibers that formed next to the hair follicles were composed of individual globular units of elastin situated adjacent to, but not integrated within, the microfibril bundles. Similarly, in the intervening dermis, globules of elastin were also observed clustered next to the microfibril bundles, however, in this locale, the globules were on average 5 times larger than those seen near the hair follicles. Based on these observations, three conclusions can be drawn. First, the fundamental mechanism that allows elastin and microfibrils to be co-localized in tissues is not dependent on fibulin-5. In the *Fbln5*$^{-/-}$ dermis, the elastin component of the elastic fiber was always observed in close proximity to the

microfibril bundle despite the absence of fibulin-5. Thus, although fibulin-5 binds both tropoelastin (Yanagisawa et al., 2002) and fibrillin-1 (Freeman et al., 2005; El-Hallous et al., 2007; Kobayashi et al., 2007), this molecular interaction is not required for the co-localization of these two major elastic fiber components in the dermis. Second, fibulin-5 is required to mediate the appropriate integration of elastin into the microfibril bundle. This role of fibulin-5 could either be by simply restricting the size of the elastin globules so that they can become incorporated into the core of the microfibril bundle or by more directly aiding in the transfer and/or linking of tropoelastin monomers onto the fibrillin-1 microfibrils at a molecular level. Finally, because of the regional disparity observed with respect to the size of the elastin globules, there must be some additional protein(s) or mechanism that is responsible for this difference.

During the formation of elastin-rich tissues, microfibril bundles appear first in development and are subsequently infiltrated with elastin (Mecham and Davis, 1994). Many elastic fiber associated proteins, in addition to fibulin-5, have been shown to play critical roles in this process based on the abnormal appearance of elastic fibers in knockout mouse models. Such proteins include emilin-1 (Zacchingna et al., 2006), LOXL-1 (Liu et al., 2004), fibulin-4 (McLaughlin et al., 2006) and LTBP-4 (Dabovic et al., 2009). In all cases, despite an aberrant assembly process, the elastin and microfibrillar components of the elastic fiber always remained apposed. It is possible, therefore, that this association is not determined by a specific protein-protein interaction but rather by the existence of defined cell surface assembly sites where the elastic fiber components are either targeted for secretion or concentrated after secretion. Indeed, fibrillin-1 binds cell-surface integrins via an RGD motif (Sakamoto et al., 1996; Bax et al., 2003) and both fibrillin-1 and tropoelastin can interact with cell-surface proteoglycans (Ritty et al., 2003; Broekelmann et al., 2005), thus validating a close association of elastic fibers components with the cell surface. Furthermore, live cell imaging has shown that the initial formation of elastin globules and their subsequent assembly into elastic fibers takes place on the cell surface (Kozel et al., 2006; Czirok et al., 2006).

Tropoelastin has the interesting ability to undergo self-assembly, reflected *in vitro* by a process termed coacervation (Cox et al., 1974; Vrhovski et al., 1997; Bellingham et al., 2003). Coacervation is a reversible phase separation event whereby a protein in solution will form a molecular aggregate dependent on temperature (Urry, 1982). *In vivo*, it is generally accepted that this property of tropoelastin is an important initial step in the formation of small coacervates of tropoelastin monomers on the cell surface. The small coacervates then coalesce or mature into slightly larger aggregates followed by transfer, integration and cross-linking within the microfibrillar scaffold (Kozel et al., 2006; Czirok et al., 2006). In the $Fbln5^{-/-}$ dermis, the large elastin globules observed adjacent to the microfibril bundles but not incorporated within the bundles suggests that, in the absence of fibulin-5, excessive coacervation or aggregation of coacervates occurred. By inference, therefore, one role of fibulin-5 would be to limit the extent of tropoelastin self-assembly, likely mediated through fibulin-5-tropoelastin interactions. Based on these observations, we recently used a well-characterized biochemical assay of tropoelastin coacervation and maturation to investigate the kinetics of tropoelastin self-assembly in the presence and absence of fibulin-5. The *in vitro* results that we obtained support the ultrastructural data and conclusions of our present study in that fibulin-5 was found have no effect on the initial coacervation process but significantly restricted the subsequent coalescence (maturation) and growth of tropoelastin aggregates (Cirulis et al., 2008).

In the present study, the ultrastructure of the elastic fibers formed in the absence of fibulin-5 differed between those fibers situated next to the hair follicles and those found in the intervening dermis, with the elastin globules in the intervening dermis being considerably larger. This observation implies that there may be a protein(s) with some redundant function near the hair follicles (epidermal cells) that is not present in the dermis at a distance from the follicles.

Recently, we have shown that fibulin-2 is functionally redundant for fibulin-5 in the assembly of the IEL in the aortic wall by generating a fibulin-2/-5 double knockout mouse (H. Yanagisawa and E.C. Davis, unpublished results). Consistent with this observation, we found that vessels in the *Fbln5*$^{-/-}$ dermis had a well-formed IEL but were absent of medial and adventitial elastic fibers. Based on these data, we propose that fibulin-2 is able to partially compensate for the function of fibulin-5 adjacent to the hair follicles and subjacent to endothelial cells in the dermal vasculature. This restricted compensatory ability of fibulin-2 is supported by its limited expression pattern which includes sites of epithelial-mesenchymal interactions, such as developing hair follicles (Zhang et al., 1996), and in the intima of blood vessels (Sicot et al., 2008), and is further supported by the demonstration of an upregulation of *Fbln2* in the skin of *Fbln5*$^{-/-}$ mice. Interestingly, *Fbln4* was also significantly upregulated in the *Fbln5*$^{-/-}$ mouse skin suggesting an additional possible compensatory protein. Based on knockout mouse studies, fibulin-4 is the most critical fibulin for normal elastic fiber assembly, with *Fbln4*$^{-/-}$ mice dying perinatally from severe lung and vascular defects as a consequence of grossly defective elastic fiber development (McLaughlin et al., 2006).

Critical to the formation of mature elastic fibers is a final cross-linking event whereby individual tropoelastin monomers are covalently cross-linked to form an insoluble elastin polymer. The initial step in this process requires oxidative deamination of lysine residues catalysed by a LOX enzyme. The subsequent steps are spontaneous and involve aldehyde condensation reactions that lead to the formation of covalent isodesmosine and desmosine cross-links that are unique to elastin (Vrhovski and Weiss, 2001). In the absence of fibulin-5, we found reduced levels of desmosine in the skin, as expected from the sparse distribution of elastic fibers seen in this tissue. The gene expression of elastin, however, was unaffected leading to the hypothesis that the process of cross-linking was defective.

Both LOX and LOXL-1 are known to play a significant role in tropoelastin cross-linking during the formation of elastic fibers as evidenced by gene ablation studies. Knockout mice deficient in LOX cannot correctly cross-link elastin or collagen and hence have major developmental defects in the lung, cardiovascular system and skin (Maki et al., 2002; Hornstra et al., 2003). These animals die perinatally from diaphragmatic and vascular rupture, most likely from impaired collagen assembly. In contrast, LOXL-1-null mice are viable (Liu et al., 2004). However, the mice do show lax skin, vascular abnormalities, enlarged airspaces and pelvic organ prolapse, consistent with aberrant elastic fiber assembly. Distinct from LOX, LOXL-1 has been shown to specifically localize to sites of elastic fiber assembly and to interact with fibulin-5 (Liu et al., 2004). For this reason, we chose to investigate the distribution and potential activity of LOXL-1 in the skin of the *Fbln5*$^{-/-}$ mice using antibodies to either an N-terminal region in the pro-peptide which would localize the inactive enzyme or cleaved pro-peptide, or to a C-terminal region that would localize both active and inactive enzyme.

In vitro studies have shown that the pro-region of LOXL-1 is necessary for its deposition and localization into elastic fibers (Thomassin et al., 2005). Based on our current findings, we now know that this localization is independent of fibulin-5. This conclusion is somewhat in conflict with the suggestion by Lui and colleagues (2004) that fibulin-5 might be responsible to tether LOXL-1 to elastic fibers. The authors based their suggestion on the absence of a fibrillar staining pattern for LOXL-1 in the dermis of *Fbln5*$^{-/-}$ mice. However, without EM analysis, the authors most likely did not realize that the elastic fibers in the dermis of the *Fbln5*$^{-/-}$ mice were abnormal and consisted of large globules of elastin and rather than fibers, as we have reported herein. Thus, the staining pattern for LOXL-1 that they observed, although not fibrillar, was most likely elastin-related.

The considerable amount of N-terminal labeling for LOXL-1 that we observed on the elastin globules in the dermis of *Fbln5*$^{-/-}$ mice, compared to the absence of N-terminal staining in

wild-type dermis, could imply that fibulin-5 either directly or indirectly plays an important role in the proteolytic processing and activation of LOXL-1. To date, there is no evidence that fibulin-5 can directly activate LOXL-1. There are, however, multiple bone morphogenetic protein 1-related mammalian metalloproteinases that are know to process pro-LOXs and control their activation (Uzel et al., 2001). It is possible, therefore, that the binding of fibulin-5 to LOXL-1 may facilitate the proteolytic activities of this group of metalloproteinases. In support of this notion, a similar functional relationship has been reported for fibronectin whereby high affinity binding of fibronectin to LOX is critical for its proteolytic activation (Fogelgren et al., 2005). These results suggest that distinct matrices may provide specific microenvironments to regulate the catalytic activity LOXs. As further support for the importance of fibulin-5 to influence the activity of LOXs, Hirai and colleagues (2007) demonstrated that exogenous fibulin-5 added to human skin fibroblast cultures had the ability to promote elastic fiber assembly but that this effect was dependent on the activation of LOXs. Thus, the exogenous fibulin-5 was not functioning simply to nucleate tropoelastin momers to the microfibrillar scaffold but rather promote its cross-linking.

In summary, we have used EM and immunolabeling techniques to reveal several roles of fibulin-5 in elastic fiber assembly that have yet been unrecognized. Based on our findings, we propose that fibulin-5 functions to restrict the aggregation (or maturation) of tropoelastin coacervates thereby allowing the incorporation of small tropoelastin assemblies into the microfibrillar bundles for subsequent cross-linking. We also suggest, with supporting evidence from our fibulin-2/-5 double knockout study (H. Yanagisawa and E.C. Davis, unpublished results) and qPCR data presented in the present study, that fibulin-2, and perhaps fibulin-4, may play compensatory roles for some of the functions of fibulin-5 in specific locales. Finally, we have shown that fibulin-5 may play an important role in the activation of LOX-1 during the ultimate step of elastin fiber formation, and additionally, that gene expression of LOX and LOXL-1 may be influenced by the presence of fibulin-5 and/or by the quality of the assembled elastic fibers.

4. EXPERIMENTAL PROCEDURES

4.1. Mice

Fibulin-5 gene knockout (*Fbln5*$^{-/-}$) mice were generated as previously described (Yanagisawa et al., 2002). For all experiments, dorsal skin from age-matched wild-type, *Fbln5*$^{+/-}$ and *Fbln5*$^{-/-}$ mice on a C57Bl6/129SvEv background was used. All studies were carried out in accordance with University Animal Care Committee regulations and protocols.

4.2. Histology

Dorsal skin from mice ranging in age from 14 days to one year was fixed in 4% buffered paraformaldehyde overnight, then dehydrated and embedded in paraffin. Five μm sections were stained by modified Hart's resorcin-fuchsin stain for elastin (Starcher et al., 2005). After staining, the slides were rinsed in water and counterstained with 0.25% metanil yellow in 0.25% acetic acid. Since the general appearance and distribution of the elastic fibers in the skin was similar at all ages, only images from young adult mice (2 months) as shown.

4.3. Desmosine analysis

Two full-thickness, 3-mm punch biopsies were obtained from skin removed from the shaved dorsum of 14 day-old mice after fixation overnight in 10% buffered formalin (n = 5 mice for each genotype). The biopsies were hydrolyzed in 500 μl 6 N HCL, evaporated, re-dissolved in 500 μl water and microfuged to remove insoluble material. For desmosine content, 50 μl was assayed by radioimmunoassay as described (Starcher and Conrad, 1995). The desmosine

content in the two biopsies from each individual animal was first averaged, and then this value used for determining the average desmosine content per genotype.

4.4. Electron microscopy

Strips of skin from the dorsum of wild-type and *Fbln5*$^{-/-}$ mice (2 months old) were trimmed into 1 × 2 mm pieces and fixed in 3% glutaraldehyde in 0.1 M sodium cacodylate (pH 7.4) overnight at 4°C. After extensive washing in 0.1 M sodium cacodylate buffer, the tissue pieces were sequentially treated with osmium tetroxide, tannic acid and uranyl acetate, then dehydrated and embedded in Epon as previously described (Davis, 1993). Thin sections (60 nm) were counterstained with methanolic uranyl acetate and lead citrate (Franc et al., 1984) and viewed using a Tecnai 12 transmission electron microscope at 120 kV. Images were digitally captured. To determine the dimensions of the elastin globules and elastin deposits observed in the dermis of the *Fbln5*$^{-/-}$ mice, high resolution (1024 × 1024 pixel) images captured at 43,000X magnification were processed for image analysis using Matlab 7.0™ with a subprogram developed to allow the quantification of morphological parameters (Nerem et al., 1981). Data was reported using box-and-whisker plots (small globules n = 39; larger deposits n = 19).

4.5. Quantitative real-time PCR

Dorsal skin was removed from 7 day-old wild-type and *Fbln5*$^{-/-}$ mice (n = 5 for each genotype) and frozen in liquid nitrogen. Each sample was separately powdered using a mortar and pestle under liquid nitrogen. To each sample, 0.8 ml of TRIzol Reagent (Invitrogen, Carlsbad, CA) was added and RNA was subsequently isolated according to manufacturer's instructions. DNase I (Invitrogen) treatment and reverse transcription were performed using 5 μg total RNA with Superscript II Reverse Transcriptase (Invitrogen) at 42°C for 50 min. Gene expression levels were quantified using SYBR-green reaction mixture (Applied Biosystems, Streetsville, ON). Each qPCR reaction contained 100 ng of cDNA diluted in RNase-free water, SYBR-green buffer and 0.5 μM forward and reverse primers (Table 1). Expression levels were analyzed using an ABI StepOne Real-Time PCR System and carried out with a thermal cycler profile of 15 sec at 95°C, 30 sec at 58°C and 30 sec at 72°C for 32 repetitions. Dissociation curve analyses were performed to show the specificity of amplification. Results were analyzed using the comparative threshold cycle (C_T) method, where ΔC_T = C_T of gene of interest minus C_T of *GAD3H* and, $\Delta\Delta C_T$ = ΔC_T of *Fbln5*$^{-/-}$ mice minus ΔC_T of wild-type mice. Relative expression was calculated as $2^{-\Delta\Delta CT}$. qPCR for each sample was run in triplicate and results expressed as the mean ± S.D. Similar data was obtained when repeated using *β-actin* for normalization (data not shown).

4.6. Immunofluorescence microscopy

Dorsal skin from 2 month-old wild-type and *Fbln5*$^{-/-}$ mice was embedded in OCT compound (Canemco, St. Laurent, QC) and stored at −80°C. Five micron frozen sections were fixed with 2% paraformaldehyde in phosphate buffered saline (PBS) for 15 min and treated with guanidine-HCl, iodoacetamide and NH_4Cl as previously described (Gibson et al., 1989). After blocking in 5% goat serum for 1 h, the sections were incubated with either a polyclonal antibody raised against recombinant mouse tropoelastin at 1:50 (generous gift from Dr. Robert P. Mecham) or with N- or C-terminal specific polyclonal antibodies to LOXL-1 at 1:200 (generous gifts from Dr. Tiansen Li). Sections were then washed and incubated with FITC-conjugated goat anti-rabbit antibody (ImmunoPure, Rockford, IL). Sections were viewed on a Axioskop light microscope and images were digitally captured using an AxioCam camera (Carl Zeiss, North York, ON).

4.7. Electron microscopy immunogold labeling

Skin was prepared and embedded in Lowicryl K4M as previously described (Davis, 1994). Briefly, skin was trimmed, fixed with 4% paraformaldehyde in 0.1 M Sorensen's buffer (pH 7.4), dehydrated in a graded series of methanol, and then infiltrated with methanol/Lowicryl K4M mixtures at progressively lower temperature to −35°C. Samples were then embedded in cold Lowicryl K4M (SPI Supplies, West Chester, PA) and polymerized by ultraviolet light at −35°C. For immunogold labeling, Lowicryl K4M sections (80 nm) were placed on formvar-coated nickel grids and blocked with 1% bovine serum albumin (BSA) in 50 mM Tris and 100 mM NaCl (pH 7.4) for 1 h. Sections were then incubated with primary antibody (anti-tropoelastin at 1:200; N- and C-terminal anti-LOXL-1 at 1:50). After 1 h and several washes, the sections were incubated with a goat $F(ab)_2$ anti-rabbit IgG conjugated to 10 nm colloidal gold (Ted Pella, Redding, CA). After labeling, sections were washed and counterstained with uranyl acetate and lead citrate.

Acknowledgments

The authors thank Dr. Robert P. Mecham (Washington University School of Medicine, St. Louis, MO) for critical review of the manuscript and for the mouse tropoelastin antibody, and Dr. Tiansan Li (Harvard University Medical School, Boston, MA) for antibodies to LOXL-1. We also thank Jeannie Mui, Lee-Anne Monaghan and Kelly Sears for EM support, Rujuan Huo, Ailian Li and Shaozhen Fang for histology preparation, and Rachel Bissonnette and Shelby Chapman for animal care. This work was supported by National Institutes of Health grant HL71157 (HY, with consortium funds to ECD), Canadian Institutes of Health grants MOP57663 and MOP86713 (ECD), Natural Sciences and Engineering Research Council of Canada grant RGPIN 35710-08 (ECD) and a Swedish Heart-Lung Foundation Fellowship (AB). ECD is a Canada Research Chair.

References

Bax DV, Bernard SE, Lomas A, Morgan A, Humphries J, Shuttleworth CA, Humphries MJ, Kielty CM. Cell adhesion to fibrillin-1 molecules and microfibrils is mediated by alpha 5 beta 1 and alpha v beta 3 integrins. J Biol Chem 2003;278:34605–34616. [PubMed: 12807887]

Bellingham CM, Lillie MA, Gosline JM, Wright GM, Starcher BC, Bailey AJ, Woodhouse KA, Keeley FW. Recombinant human elastin polypeptides self-assemble into biomaterials with elastin-like properties. Biopolymers 2003;70:445–455. [PubMed: 14648756]

Broekelmann TJ, Kozel BA, Ishibashi H, Werneck CC, FWK, Zhang L, Mecham RP. Tropoelastin interacts with cell-surface proteoglycans via its COOH-terminal domain. J Biol Chem 2005;280:40939–40947. [PubMed: 16192266]

Buechner SA, Itin P. Papular elastorrhexis. Report of five cases. Dermatology 2002;205:198–200. [PubMed: 12218247]

Cox BA, Starcher BC, Urry DW. Coacervation of tropoelastin results in fiber formation. J Biol Chem 1974;249:997–998. [PubMed: 4359779]

Cirulis JT, Bellingham CM, Davis EC, Hubmacher D, Reinhardt DP, Mecham RP, Keeley FW. Fibrillins, fibulins, and matrix-associated glycoprotein modulate the kinetics and morphology of in vitro self-assembly of a recombinant elastin-like polypeptide. Biochemistry 2008;47:12601–12613. [PubMed: 18973305]

Czirok A, Zach J, Kozel BA, Mecham RP, Davis EC, Rongish BJ. Elastic fiber macro-assembly is a hierarchical, cell motion-mediated process. J Cell Physiol 2006;207:97–106. [PubMed: 16331676]

Dabovic B, Chen Y, Choi J, Vassallo M, Dietz HC, Ramirez F, von Melchner H, Davis EC, Rifkin DB. Dual functions for LTBP in lung development: LTBP-4 independently modulates elastogenesis and TGF-beta activity. J Cell Physiol 2009;219:14–22. [PubMed: 19016471]

Dahlback K, Ljungquist A, Lofberg H, Dahlback B, Envall E, Sakai LY. Fibrillin immunoreactive fibers constitute a unique network in the human dermis. J Invest Dermatol 1990;94:284–291. [PubMed: 1689758]

Davis EC. Smooth muscle cell to elastic lamina connections in the developing mouse aorta: Role in aortic medial organization. Lab Invest 1993;68:89–99. [PubMed: 8423679]

Davis EC. Immunolocalization of microfibril and microfibril-associated proteins in the subendothelial matrix of the developing mouse aorta. J Cell Sci 1994:727–736. [PubMed: 8006086]

Davis EC, Blattel SA, Mecham RP. Remodeling of elastic fiber components in scleroderma skin. Connect Tiss Res 1999;40:113–121.

El-Hallous E, Sasaki T, Hubmacher D, Getie M, Tiedemann K, Brinckmann J, Bätge B, Davis EC, Reinhardt DP. Fibrillin-1 interactions with fibulins depends on the first hybrid domain and provide an adaptor function to tropoelastin. J Biol Chem 2007;282:8935–8946. [PubMed: 17255108]

Fogelgren B, Polgár N, Szauter KM, Ujfaludi Z, Laczkó R, Fong KS, Csiszar K. Cellular fibronectin binds to lysyl oxidase with high affinity and is critical for its proteolytic activation. J Biol Chem 2005;280:24690–24697. [PubMed: 15843371]

Franc S, Garrone R, Bosch A, Franc JM. A routine method for contrasting elastin at the ultrastructural level. J Histochem Cytochem 1984;32:251–258. [PubMed: 6198356]

Freeman LJ, Lomas A, Hodson N, Sherratt MJ, Mellody KT, Weiss AS, Shuttleworth A, Kielty CM. Fibulin-5 interacts with fibrillin-1 molecules and microfibrils. Biochem J 2005;388:1–5. [PubMed: 15790312]

Gibson MA, Kumaratilake JS, Cleary EG. The protein components of the 12-nanometer microfibrils of elastic and non-elastic tissues. J Biol Chem 1989;264:4590–4598. [PubMed: 2647740]

Giro MG, Duvic M, Smith LT, Kennedy R, Rapini R, Arnett FC, Davidson JM. Buschke-Ollendorff syndrome associated with elevated elastin production by affected skin fibroblasts in culture. J Invest Dermatol 1992;99:129–137. [PubMed: 1629625]

Hennekam RC. Costello syndrome: an overview. Am J Med Genet 2003;117(C):42–48.

Hirai M, Ohbayashi T, Horiguchi M, Okawa K, Hagiwara A, Chien KR, Kita T, Nakamura T. Fibulin-5/DANCE has an elastogenic organizer activity that is abrogated by proteolytic cleavage in vivo. J Cell Biol 2007;176:1061–1071. [PubMed: 17371835]

Hirano E, Knutsen RH, Sugitani H, Ciliberto CH, Mecham RP. Functional rescue of elastin insufficiency in mice by the human elastin gene. Circ Res 2007;101:523–531. [PubMed: 17626896]

Hornstra IK, Birge S, Starcher B, Bailey AJ, Mecham RP, Shapiro SD. Lysyl oxidase is required for vascular and diaphragmatic development in mice. J Biol Chem 2003;278:14387–14393. [PubMed: 12473682]

Kagan, HM. Characterization and regulation of lysyl oxidase. In: Mecham, RP., editor. Regulation of Matrix Accumulation. Academic Press; New York: 1986. p. 321-398.

Kagan HM, Trackman PC. Properties and function of lysyl oxidase. Am J Respir Cell Mol Biol 1991;5:206–210. [PubMed: 1680355]

Kielty CM. Elastic fibers in health and disease. Expert Rev Mol Med 2006;8:1–23. [PubMed: 16893474]

Kobayashi N, Kosta G, JHOG, Keene DR, Bächinger HP, Hanisch FG, Markova D, Tsuda T, Timpl R, Chu ML, Sasaki T. A comparative analysis of the fibulin protein family. Biochemical characterization, binding interactions, and tissue localization. J Biol Chem 2007;282:11805–11805. [PubMed: 17324935]

Kowal RC, Richardson JA, Miano JM, Olson EN. EVEC, a novel epidermal growth factor-like repeat-containing protein upregulated in embryonic and diseased adult vasculature. Circ Res 1999;84:1166–1176. [PubMed: 10347091]

Kozel BA, Wachi H, Davis EC, Mecham RP. Domains in tropoelastin that mediate elastin deposition *in vitro* and *in vivo*. J Biol Chem 2003;278:18491–18498. [PubMed: 12626514]

Kozel BA, Rongish BJ, Czirok A, Zach J, Little CD, Davis EC, Knutsen RH, Wagenseil JE, Levy MA, Mecham RP. Elastic fiber formation: a dynamic view of extracellular matrix assembly using timer reporters. J Cell Physiol 2006;207:87–96. [PubMed: 16261592]

Liu X, Zhao Y, Gao J, Pawlyk B, Starcher B, Spencer JA, Yanagisawa H, Zuo J, Li T. Elastic fiber homeostasis requires lysyl oxidase-like 1 protein. Nat Genet 2004;36:178–182. [PubMed: 14745449]

Lomas AC, Mellody KT, Freeman LJ, Bax DV, Shuttleworth CA, Kielty CM. Fibulin-5 binds human smooth-muscle cells through alpha5beta1 and alpha4beta1 integrins, but does not support receptor activation. Biochem J 2007;405:417–428. [PubMed: 17472576]

Maki JM, Rasanen J, Tikkanen H, Sormunen R, Makikallio K, Kivirikko KI, Soininen R. Inactivation of the lysyl oxidase gene LOX leads to aortic aneurysms, cardiovascular dysfunction, and perinatal death in mice. Circulation 2002;106:2503–2509. [PubMed: 12417550]

McLaughlin PJ, Chen Q, Horiguchi M, Starcher BC, Stanton JB, Broekelmann TJ, Marmorstein AD, McKay B, Mecham R, Nakamura T, Marmorstein LY. Targeted disruption of fibulin-4 abolishes elastogenesis and causes perinatal lethality in mice. Mol Cell Biol 2006;26:1700–1709. [PubMed: 16478991]

Mecham, RP.; Davis, EC. Elastic Fiber Structure and Assembly. In: Yurchenko, PD.; Birk, DE.; Mecham, RP., editors. Extracellular Matrix Assembly and Structure. Academic Press; San Diego: 1994. p. 281-314.

Nakamura T, Ruiz-Lozano P, Ikeda Y, Iwanaga Y, Hinek A, Minamisawa S, Cheng CF, Kobuke K, ND, Takada Y, Tashiro K, Ross J, Honjo T, Chien KR. Fibulin-5/DANCE is essential for elastogenesis *in vivo*. Nature 2002;415:171–175. [PubMed: 11805835]

Nakamura T, Ruiz-Lozano P, Lindner V, Yabe D, Taniwaki M, Furukawa Y, Kobuke K, Tashiro K, Lu Z, Andon NL, Schaub R, Matsumori A, Sasayama S, Chien KR, Honjo T. DANCE, a novel secreted RGD protein expressed in developing, atherosclerotic, and balloon-injured arteries. J Biol Chem 1999;274:22476–22483. [PubMed: 10428823]

Nerem RM, Levesque MJ, Cornhill JF. Vascular endothelial morphology as an indicator of the pattern of blood flow. J Biomech Eng 1981;103:172–176. [PubMed: 7278195]

Parks, WC.; Pierce, RA.; Lee, KA.; Mecham, RP. Elastin. In: Bittar, EE.; Kleinman, HK., editors. Advances in Cell and Molecular Biology. JAI Press Inc; Greenwich: 1993. p. 133-182.

Patroi I, Annessi G, Girolomoni G. Mid-dermal elastolysis: a clincal, histological, and immunohistochemical study of 11 patients. J Am Acad Dermatol 2003;48:846–851. [PubMed: 12789173]

Ritty TM, Broekelmann TJ, Werneck CC, Mecham RP. Fibrillin-1 and -2 contain heparin-binding sites important for matrix deposition and that support cell attachment. Biochem J 2003;375:425–432. [PubMed: 12837131]

Rosenbloom J, Abrams WR, Mecham RP. Extracellular matrix 4: The elastic fiber. Faseb J 1993;7:1208–1218. [PubMed: 8405806]

Sakamoto H, Broekelmann T, Cheresh DA, Ramirez F, Rosenbloom J, Mecham RP. Cell-type specific recognition of RGD- and non RGD-containing cell binding domains in fibrillin-1. J Biol Chem 1996;271:4916–4922. [PubMed: 8617764]

Sicot FX, Tsuda T, Markova D, Klement JF, Arita M, Zhang RZ, Pan TC, Mecham RP, Birk DE, Chu ML. Fibulin-2 is dispensable for mouse development and elastic fiber formation. Mol Cell Biol 2008;28:1061–1067. [PubMed: 18070922]

Spencer JA, Hacker SL, Davis EC, Mecham RP, Knustsen RH, Li DY, Gerard RD, Richardson JA, Olson EN, Yanagisawa H. Altered vascular remodeling in fibulin-5-deficient mice reveals a role of fibulin-5 in smooth muscle cell proliferation and migration. Proc Natl Acad Sci USA 2005;102:2946–2951. [PubMed: 15710889]

Starcher B, Aycock RL, Hill CH. Multiple roles for elastic fibers in the skin. J Histochem Cytochem 2005;53:431–443. [PubMed: 15805418]

Starcher BC, Conrad M. A role for neutrophil elastase in the progression of solar elastosis. Connect Tiss Res 1995;31:133–140.

Sullivan KM, Bissonnette R, Yanagisawa H, Hussain SN, Davis EC. Fibulin-5 functions as an endogenous angiogenesis inhibitor. Lab Invest 2007;87:818–827. [PubMed: 17607303]

Thomassin L, Werneck CC, Broekelmann TJ, Gleyzal C, Hornstra IK, Mecham RP, Sommer P. The pro-regions of lysyl oxidase and lysyl oxidase-like 1 are required for deposition onto elastic fibers. J Biol Chem 2005;280:42848–42855. [PubMed: 16251195]

Uitto, J.; Pulkkinen, L. Heritable diseases affecting the elastic tissue: cutis laxa, pseudoxanthoma elasticum and related disorders. In: Rimoin, DL.; Connor, JM.; Pyeritz, RE.; Korfs, BR., editors. Rimoin's Principles and Practices of Medical Genetics. Churchill Livingstone; New York: 2002. p. 4044-4068.

Uitto J, Pulkkinen L, Ringfeil F. Molecular genetics of pseudoxanthoma elasticum: a metabolic disorder at the environment-genome interface? Trends Mol Med 2001;7:13–17. [PubMed: 11427982]

Urban Z, Gao J, Pope FM, Davis EC. Autosomal dominant cutis laxa with severe lung disease: Synthesis and matrix deposition of mutant tropoelastin. J Invest Dermatol 2005;124:1193–1199. [PubMed: 15955094]

Urry DW. Characterization of soluble peptides of elastin by physical techniques. Methods Enzymol 1982;82:673–716. [PubMed: 7078453]

Uzel MI, Scott IC, Babakhanlou-Chase H, Palamakumbura AH, Papano WN, Hong HH, Greenspan DS, Trackman PC. Multiple bone morphogenetic protein 1-related mammalian metalloproteinases process pro-lysyl oxidase at the correct physiological site and control lysyl oxidase activation in mouse embryo fibroblast cultures. J Biol Chem 2001;276:22537–22543. [PubMed: 11313359]

Vrhovski B, Jensen S, Weiss AS. Coacervation characteristics of recombinant human tropoelastin. Eur J Biochem 1997;250:92–98. [PubMed: 9431995]

Vrhovski B, Weiss AS. Biochemistry of tropoelastin. Eur J Biochem 2001;258:1–18. [PubMed: 9851686]

Yanagisawa H, Davis EC, Starcher BC, Ouchi T, Yanagisawa M, Richardson JA, Olson EN. Fibulin-5 is an elastin-binding protein essential for elastic fibre development *in vivo*. Nature 2002;415:168–171. [PubMed: 11805834]

Yen A, Wen J, Grau M, Sanchez RL, Smith EB. Elastoderma. J Am Acad Dermatol 1995;33:389–392. [PubMed: 7615893]

Zacchingna L, Vecchione C, Notte A, Cordenonsi M, Dupont S, Maretto S, Cifelli G, Ferrari A, Maffei A, Fabbro C, Braghetta P, Marino G, Selvetella G, Aretini A, Colonnese C, Bettarini U, Russo G, Soligo S, Adorno M, Bonaldo P, Volpin D, Piccolo S, Lembo G, Bressan GM. Emilin1 links TGF-beta maturation to blood pressure homeostasis. Cell 2006;124:929–942. [PubMed: 16530041]

Zhang HY, Timpl R, Sasaki T, Chu ML, Ekblom P. Fibulin-1 and fibulin-2 expression during organogenesis in the developing mouse embryo. Dev Dyn 1996;205:348–364. [PubMed: 8850569]

Zheng Q, Davis EC, Richardson JA, Starcher BC, Li T, Gerard RD, Yanagisawa H. Molecular analysis of fibulin-5 function during de novo synthesis of elastic fibers. Mol Cell Biol 2007;27:1083–1095. [PubMed: 17130242]

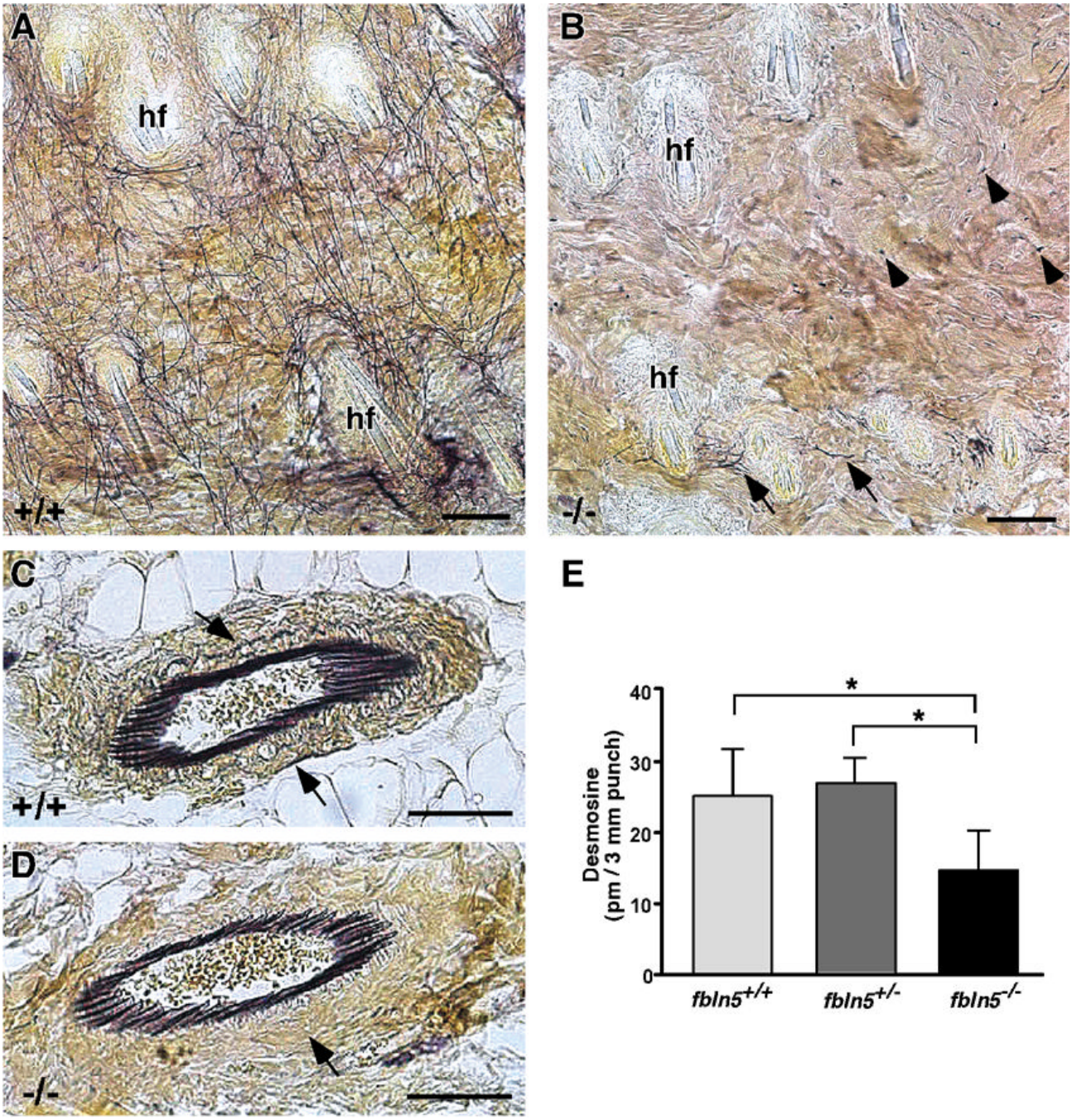

Figure 1. Elastin distribution in *en face* sections of dermis and desmosine analysis

In 2 month-old wild-type skin (**A**), an extensive elastic fiber network (black lines) can be seen between the hair follicles (hf). In fibulin-5 null skin (**B**), only a few intact elastic fibers (arrows) can be seen near the hair follicles (hf). Distant to the hair follicles, very small foci of elastin-positive staining are evident (arrowheads). In contrast to the dermis, small blood vessels near the hypodermis appear similar between wild-type (**C**) and fibulin-5 null (**D**) skin. Closer examination, however, does show a difference in the elastic fiber distribution in the surrounding media and adventitia (**C, D** - arrows). Desmosine analysis of 14 day-old mouse skin shows a significant decrease in amount of desmosine, a measure of mature cross-linked elastin, in

Fbln5$^{-/-}$ skin compared to wild-type or *Fbln5*$^{+/-}$ skin (means ± S.D.; * = $p < 0.05$; n = 5 for each genotype). Scale bars = 50 μm.

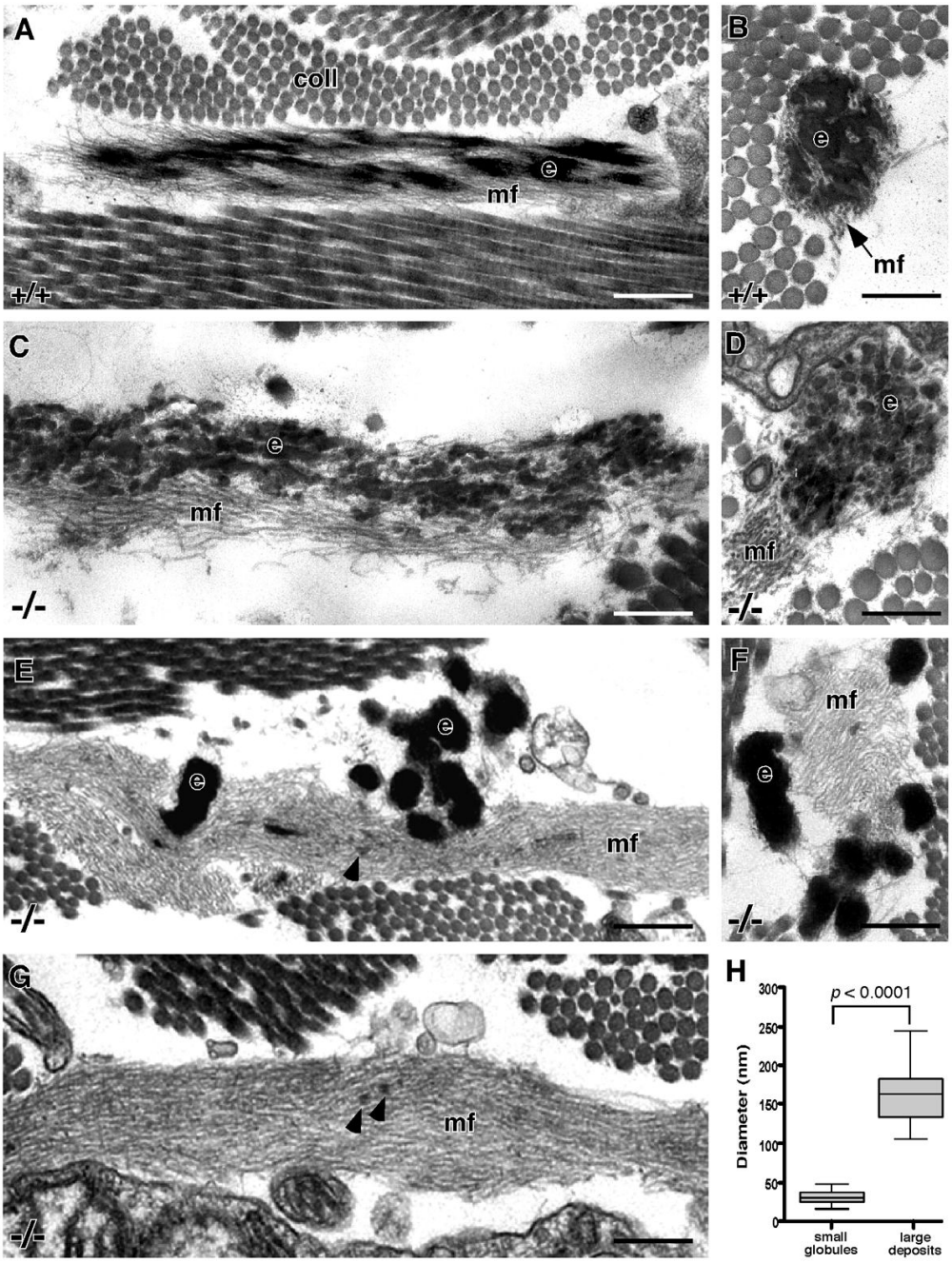

Figure 2. Electron micrographs of dermal elastic fibers in wild-type and fibulin-5 null mouse skin

Elastic fibers in wild-type skin show a solid core of elastin (e) intergrated into a bundle of microfibrils (mf) (**A** - longitudinal section, **B** - cross-section). In contrast, the elastic fibers in fibulin-5 null skin located near the hair follicles are composed of a series of small elastin globules (e) lying adjacent to the microfibrils (mf) (**C** - longitudinal section, **D** - cross-section). At a distance from the hair follicles, the small globules are replaced by larger elastin deposits (e) located outside extensive bundles of microfibrils (mf) (**E** - longitudinal section, **F** - cross-section). Microfibril bundles are also seen devoid of elastin (**G**). A few small globules of elastin can also be observed within the microfibril bundles on occasion (**E**, **G** - arrowheads). Quantification of the dimensions of the small elastin globules (n = 39) and larger elastin

deposits (n = 19) show a significant difference in size and a more uniform diameter of the small globules (**H**). The plot shows the median, 25^{th} and 75^{th} percentiles, and the maximum and minimum values. Scale bar = 0.25 μm, coll = collagen.

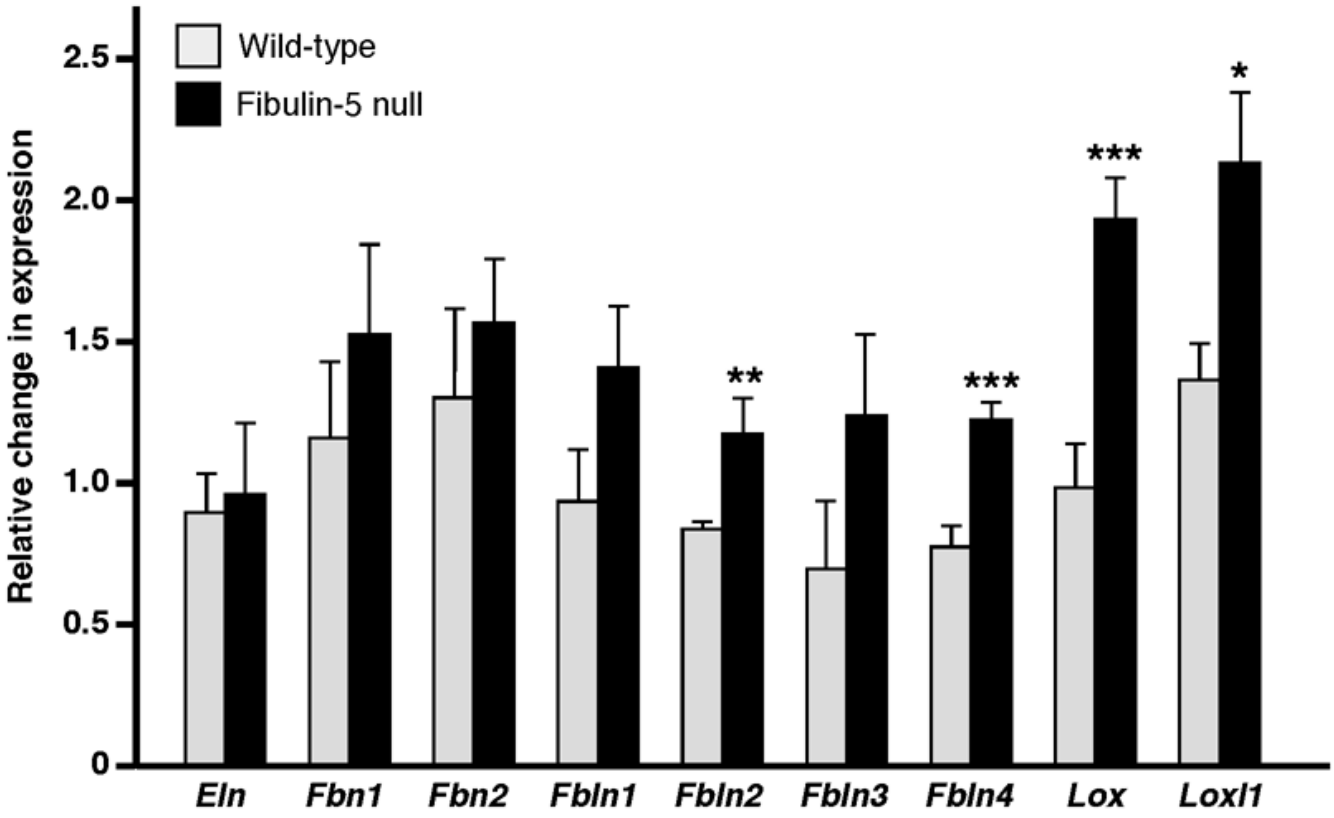

Figure 3. Quantitative real-time PCR analysis of gene expression of elastic fiber components in 7 day-old mouse skin

No significant difference in gene expression was observed between wild-type and *Fbln5*$^{-/-}$ skin for elastin (*Eln*), fibrillin-1 and -2 (*Fbn1* and *Fbn2*), and fibulin-1 and -3 (*Fbln1* and *Fbln3*). In contrast, genes encoding fibulin-2 and -4 (*Fbln2* and *Fbln4*), and lysyl oxidase (*Lox*) and lysyl oxidase like-1 (*Loxl1*) were significantly upregulated in the absence of fibulin-5 (means ± S.D.; * = $p < 0.05$, ** = $p < 0.01$, *** = $p < 0.005$; n = 5 for each genotype).

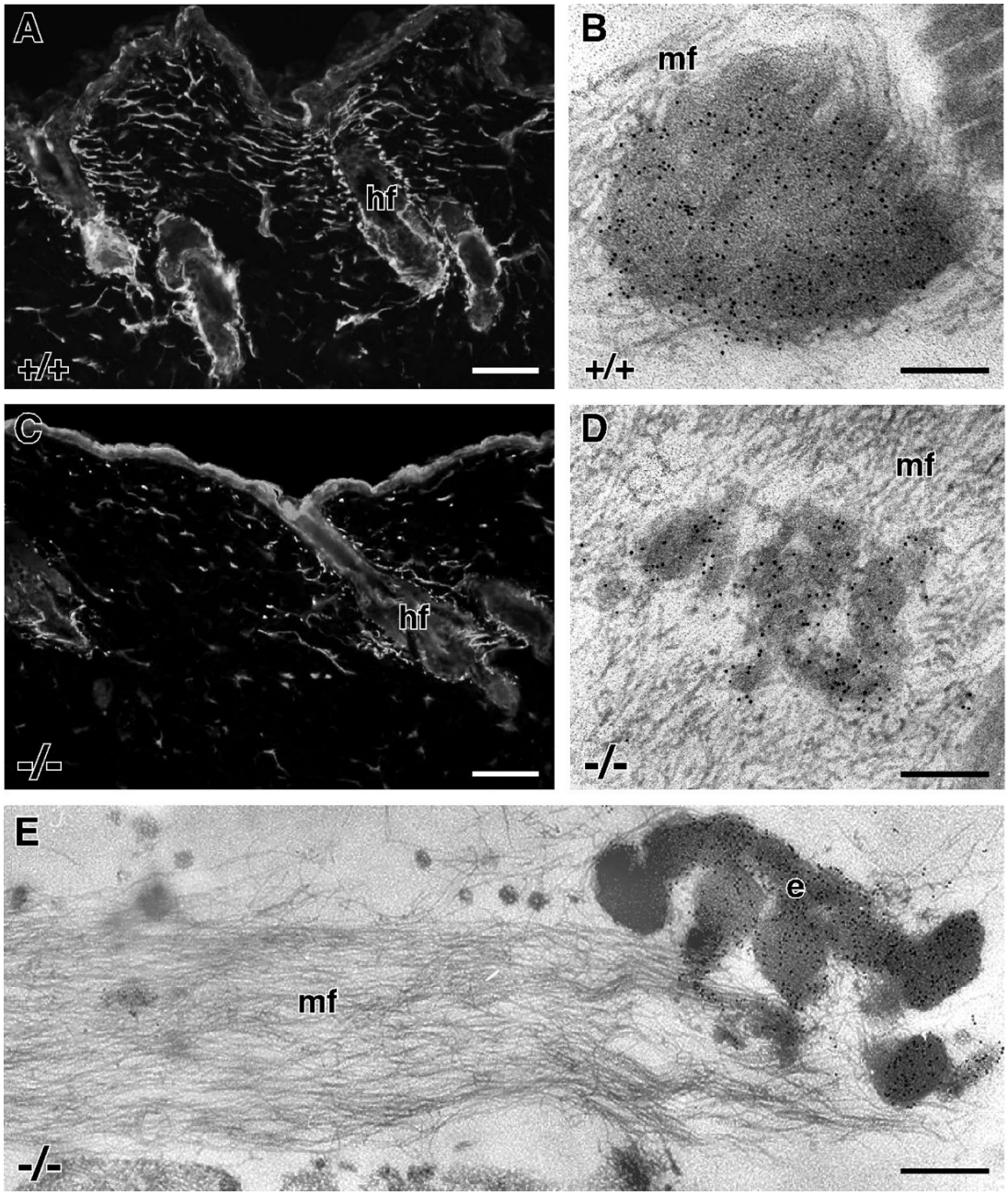

Figure 4. Tropoelastin localization in mouse skin

In wild-type mice, immunofluorescence localization of elastin at the light microscope level shows a network of elastic fibers spanning between hair follicles (**A**). Immunogold electron microscope localization of tropoelastin shows gold particles decorating the core of the elastic fiber with no gold particles labeling the peripheral microfibrils (mf) (**B**). In *Fbln5*$^{-/-}$ skin, stunted elastic fibers are seen near the hair follicles (hf) and foci of elastin staining are seen in the intervening dermis (**C**). By electron microscopy, gold particle labeling shows the presence of tropoelastin only in the small elastin globules (**D**) and larger elastin deposits (**E**), with no tropoelastin detected on the adjacent microfibrils (mf). Note that the fluorescence of the epidermis is non-specific. Scale bars = 100 μm (A, C), 0.15 μm (B, D), 0.30 μm (E).

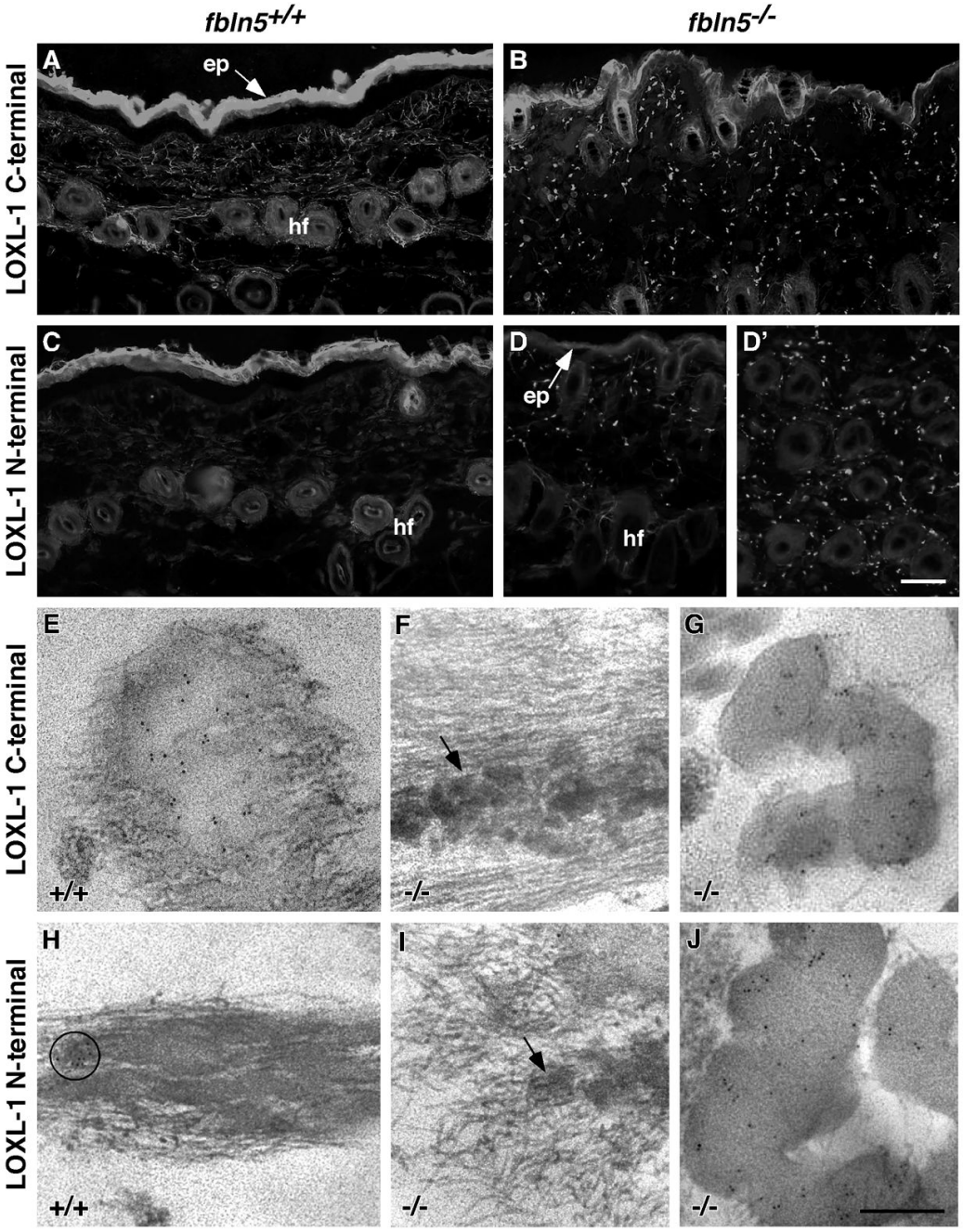

Figure 5. LOXL-1 localization in mouse skin

Wild-type and *Fbln5*$^{-/-}$ skin sections were immunolabeled at the light and electron microscope levels using a C-terminal LOXL-1 antibody that recognizes both the active and inactive forms of LOXL-1 and an N-terminal LOXL-1 antibody that recognizes only the inactive form. Immunolabeling with the C-terminal antibody shows LOXL-1 staining in filamentous network between adjacent hair follicles (hf) and within the papillary dermis between the hair follicles and epidermis (ep) in wild-type skin (**A**) and a punctate staining pattern in the *Fbln5*$^{-/-}$ skin (**B**). Wild-type skin shows no immunostaining for the N-terminus of LOXL-1 in wild-type skin (**C**), whereas a punctate staining is observed in the *Fbln5*$^{-/-}$ skin, both between the epidermis (ep) and hair follicles (hf) (**D**) and deeper in the dermis between the individual hair follicles

(**D′**). Immunofluorescence of the epidermis is non-specific. Immunogold electron microscopy using the C-terminal antibody shows gold particles on the edges of the elastin core of the elastic fibers and where the microfibrils were embedded within the core in wild-type skin (**E**). In *Fbln5*$^{-/-}$ skin, no labeling is seen on the small elastin globules (**F**), but considerable gold particles are seen to decorate the large elastin deposits (**G**). Only the occasional, rare patch of gold particles was seen on elastic fibers in wild-type skin for the N-terminus of LOXL-1 (**H** - circle). No immunogold labeling for the N-terminus of LOXL-1 was seen on the small elastin globules in the *Fbln5*$^{-/-}$ skin (**I**), however, abdundant gold particles localize to the larger elastin deposits (**J**). Scale bars = 100 μm (A–D), 0.3 μm (E–J).

Table 1

Primer sequences and product size for qPCR

GENE	FORWARD PRIMER	REVERSE PRIMER	SIZE (bp)
Eln	AACAAAGGAAGCCTAGAGCCAGTG	GATTGTGCTTAGGTCCTCATGCCT	250
Fbn1	CCAGGATACTTCCGGATAGG	CTCACGTTGGCTTCCATCTC	650
Fbn2	GGCTGCCAGAATATCCTGGGGGG	GAGCTTCTTCTTGGCCGTG	400
Fbln1	ATGGAGGCTTGCTGCACGGA	ACTGCTGCTTACAGGGC	500
Fbln2	ATTGCACAGGTGCTGAGTGT	TGGACGGTATGGCCAGCA	550
Fbln3	TACGCACTCCTTCGCTGCCC	CAGCTACAGTCCCAGTGGT	400
Fbln4	TGTGAGCAGCGCTGCTTCAA	GCAGCGGTTGTCTGACACTT	400
Lox	ACCGTGGTCTAGCTTTCCTAGTTC	GGACGTTGGGTAGCTGGGAATAAA	400
Loxl1	TTACCACAGCATGGACGAGTTCAG	GTTATGTCGATCCACTGGCAGTCA	250
GAD3H	TGGATTTGGACGCATTGGTC	TTTGCACTGGTACGTGTTGAT	210
βactin	GTATGCCTCGGTCGTACCA	CTTCTGCATCCTGTCAGCAA	500